CrossMark

ORIGINAL ARTICLE

Insect-type MEMS microrobot with mountable bare chip IC of artificial neural networks

Ken Saito[1] · Kazuki Sugita[1] · Yuki Ishihara[1] · Kei Iwata[1] · Yohei Asano[1] ·
Yuki Okane[1] · Satoko Ono[1] · Satohiro Chiba[1] · Minami Takato[1] · Fumio Uchikoba[1]

Abstract This paper discussed insect-type MEMS microrobot system which could locomote without using computer programs. Locomotion of the MEMS microrobot was generated using the analog circuit of artificial neural networks. We constructed the artificial neural networks as a bare chip integrated circuit (IC) which could mount on top of the MEMS microrobot. As a result, the MEMS microrobot system could perform the locomotion using constructed bare chip IC of artificial neural networks. The insect-type MEMS microrobot system was 0.079 g in weight and less than 5.0 mm in size. Only the power source was outside of the robot. In addition, we analyze the heat conduction of the shape memory alloy-type actuator. It was shown that the heat of shape memory alloy conducts to the mechanical parts of the MEMS microrobot; therefore, locomotion becomes slowly after 30 s. The slow locomotion was 2 mm/min. We constructed the less conduction shape memory alloy-type actuator. The locomotion speed of the insect-type MEMS microrobot using less conduction shape memory alloy-type actuator was 90.8 mm/min.

Keywords MEMS · Microrobot · Bare chip · Integrated circuit · Artificial neural networks · Shape memory alloy

✉ Ken Saito
   kensaito@eme.cst.nihon-u.ac.jp
   http://www.eme.cst.nihon-u.ac.jp/~uchikoba/

[1] Nihon University, 7-24-1 Narashinodai, Funabashi-shi, Chiba 274-8501, Japan

1 Introduction

Many types of microrobot had been proposed for several applications [1–5]. In particular, microrobot could play an important role in paramedical use such as cleaning inside the blood vessel. However, a thin artery of human is about 5 mm and artery structure of human differs greatly in individuals. Therefore, further miniaturizations and higher functionalization on the microrobot system are required to play an important role in paramedical use. Although the miniaturization of the robot has conventionally been progressed by mechanical machining and assembling, some difficulty has appeared to achieve further miniaturizations, in particular, frame parts, actuators, motion controllers, power sources, and sensors [6]. Instead of the conventional mechanical machining, microfabrication technology based on the integrated circuit (IC) production lines has been studied for making the simple and planar structure components of the microrobot [7, 8]. In addition, the development of the actuator is important subjects. The type of the microactuator by microfabrication technology is categorized into two groups: for example, uses the field forces; otherwise, uses the property of the material itself [9–13]. In particular, shape memory alloy actuator shows a large displacement such as 50 % of the total length in millimeter size. However, microactuators using field forces or piezoelectric elements to the microrobot had a weakness for moving on the uneven surface. Therefore, microrobot which could locomote by step pattern was desired.

Programmed control by digital systems based on microcontroller has been the dominant system among the microrobot control. On the other hand, insects realize the autonomous operation using excellent structure and active neural networks control by compact advanced systems. Therefore, some advanced studies of artificial neural networks have

been paid attention for applying to the robot systems. A lot of studies have reported both on software models and hardware models [14–16]. However, using the mathematical neuron models in large-scale artificial neural networks is difficult to process in continuous time because the computer simulation is limited by the computer performance, such as the processing speed and memory capacity. In contrast, using the hardware neuron model is advantageous because even if a circuit scale becomes large, the nonlinear operation can perform at high speed and process in continuous time. Therefore, the construction of a hardware neuron model which can generate oscillatory patterns was desired.

We are studying about microrobot system which could locomote by step pattern. In addition, we are constructing the artificial neural networks which could generate the locomotion of the robot. 4.0, 4.0, 3.5 mm, width, length, and height size microrobot and artificial neural networks constructed by discrete circuit board were reported in the previous work [17]. The microrobot had downsized as 4.0, 2.7, 2.5 mm, width, length, and height in size in the previous work [18]. In addition, artificial neural networks were constructed by an integrated circuit (IC) for the purpose of circuit scale down. However, previous IC chip of artificial neural networks needs a peripheral circuit to drive the shape memory alloy-type actuator. The peripheral circuit consisted by an operational amplifier for buffer and transistors for electric current amplify. The weight of the IC with peripheral circuit was 0.31 g where the weight of the MEMS microrobot was 0.02 g. Therefore, the IC with peripheral circuit was too heavy to locomote the MEMS microrobot system [19].

In this paper, we will discuss bare chip IC of artificial neural networks which can mount on the insect-type MEMS microrobot. Firstly, a micro-mechanical system of the MEMS microrobot which was fabricated by microfabrication technology was shown briefly. Secondly, a micro-electro system of the MEMS microrobot which was locomotion rhythm generator using artificial neural networks constructed by IC technology was discussed. It is necessary to downsizing and lightening the peripheral circuit to mount on the insect-type MEMS microrobot. We discuss integration of the peripheral circuits into the IC chip. Finally, we will show the locomotion of the insect-type MEMS microrobot system. In addition, we analyze the heat conduction of the shape memory alloy-type actuator.
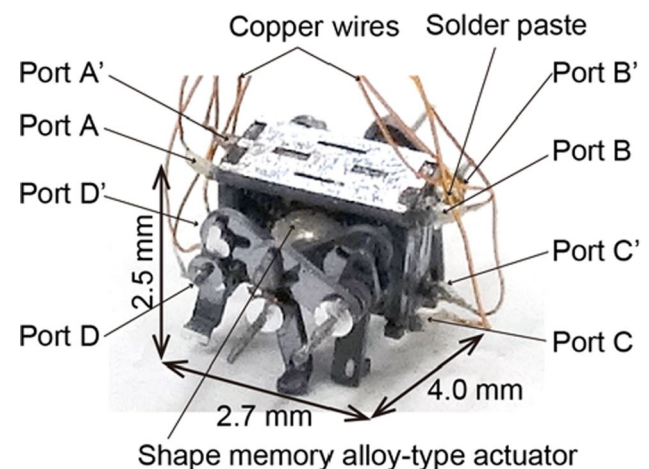
2 Micro-mechanical systems

We constructed the micro-mechanical system of the MEMS microrobot using microfabrication technology. The shapes were machined by photolithography-based inductively coupled plasma (ICP) dry etching [20]. The number of the legs of the microrobot was six. The structure and the step pattern of the robot were emulated those of an ant. The microrobot consisted of small size shape memory alloy-type actuators, body frame, link mechanisms and six legs.

Figure 1 shows the micro-mechanical system of the MEMS microrobot system. The size of the microrobot was 4.0, 2.7, 2.5 mm, width, length, and height, respectively. The copper wires above the microrobot were two GND wires and eight signal wires. The one side of the shape memory alloy connected to the copper wires and the other side connected to the shape memory alloy-type actuator using solder paste. The shape memory alloy-type actuator uses the shape memory alloy to generate the rotational movement of the actuator. The shape memory alloy can change in length according to the temperature [21, 22]. In this study, the length of the shape memory alloy was changed by supplying or stopping the current flow. We named each signal wire port as shown in the figure (Port A, B, C and D for the right side. Port A′, B′, C′ and D′ for the left side). In the case of connecting the signal wires to the bare chip IC of artificial neural networks, the microrobot could locomote. Ants can locomote smoothly on the uneven surface using step pattern. On the other hand, many microrobots were weak in moving on the uneven surface.

We replicate the locomotion of an ant using shape memory alloy-type actuators and link mechanism. To heat the shape memory alloy, it is required to input the pulse width 0.5 s, pulse period 2 s and pulse amplitude 75 mA. Therefore, the microrobot required 2 s to finish the one cycle locomotion (please see [18, 19] for more detail of micro-mechanical system of the microrobot).

Fig. 1 The micro-mechanical system of the MEMS microrobot system

3 Micro-electro systems

We designed the bare chip IC of artificial neural networks as a micro-electro system. Previous IC was voltage output; therefore, an operational amplifier for buffer and transistors for electric current amplify was used to drive the shape memory alloy-type actuator. The peripheral circuit was too heavy to locomote the microrobot system [19]. Proposing IC of artificial neural networks is current output; therefore, bare chip IC can drive the shape memory alloy-type actuator directly.

3.1 Basic components

Figure 2 shows the circuit diagram of the pulse-type hardware neuron model which is the basic component of the artificial neural networks. The pulse-type hardware neuron model consists of a synaptic model and a cell body model. Figure 2a shows the circuit diagram of the inhibitory synaptic model and Fig. 2b shows the circuit diagram of the cell body model, respectively. The cell body model has same basic features of biological neurons, such as threshold, refractory period, and spatio-temporal summation characteristics, and enables the generation of a continuous pulse wave. The synchronization phenomena of cell body model change by the connection of the synaptic model. The cell body model connected by excitatory synaptic model causes the in-phase synchronization. The cell body model connected by inhibitory synaptic model causes the anti-phase synchronization. Therefore, we use the inhibitory mutual coupling to generate the driving pulses which can operate the actuators of the microrobot. The circuit parameters of the synaptic model were as follows: $C_{IS} = 1$ pF, M_{IS1-5}: $W/L = 1$ (where W is an effective channel width and L is an effective channel length of the MOSFET, respectively). The voltage source $V_{ISDD} = 5$ V. The circuit parameters of the cell body model were as follows: $C_G = 39$ μF, $C_M = 270$ nF, M_{C1}, M_{C2}: $W/L = 10$, M_{C3}: $W/L = 0.1$, M_{C4}: $W/L = 0.3$. The voltage source $V_A = 3.3$ V. The input voltage v_{ISin} of the synaptic model was output voltage v_{Cout} of
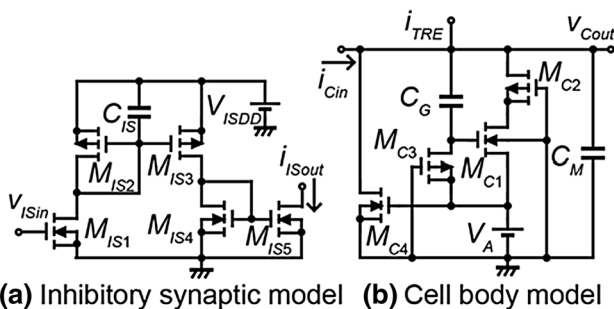
the other cell body model. The input current i_{Cin} of the cell body model was output current i_{ISout} of the synaptic model.

3.2 Artificial neural networks

Using the anti-phase synchronization phenomena, we designed the artificial neural networks. The connection diagram of designed artificial neural networks is shown in Fig. 3. Four cell body models are mutually coupled by 12 inhibitory synaptic models. Four output ports were extracted from artificial neural networks. In addition, four trigger pulse input port were extracted from artificial neural networks. According to the input timing of single external trigger pulse, artificial neural networks could change the sequence of driving pulses.

Layout pattern of the artificial neural networks is shown in Fig. 4. The design rule of the IC was 4 metal 2 poly CMOS 0.35 μm. The chip was a square 2.45 mm × 2.45 mm in size. Connections of artificial neural networks were same as shown in Fig. 3.

3.3 Current output circuit

The cell body models are voltage output. Therefore, we convert the voltage to current for actuating the shape memory alloy-type actuators. Therefore, the operational amplifier and the transistors which were used as the peripheral circuit in the previous study [19] can be simplified.
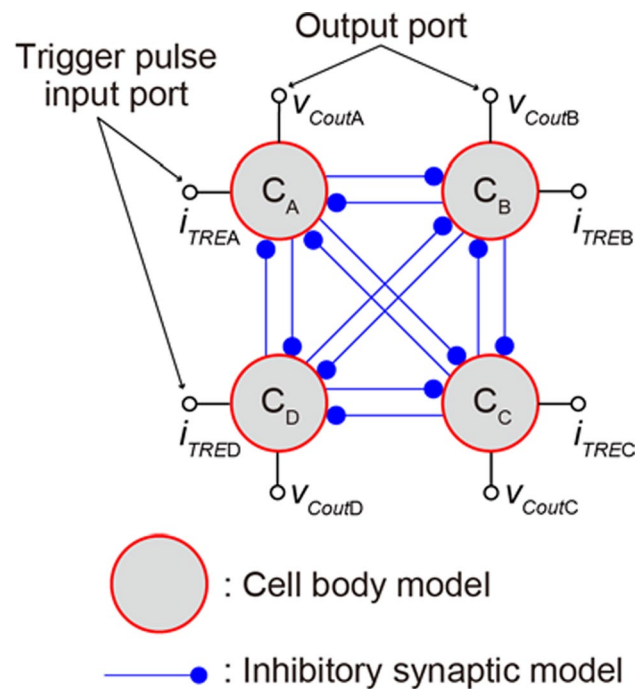

Fig. 2 The circuit diagram of the pulse-type hardware neuron model

Fig. 3 Connection diagram of designed artificial neural networks
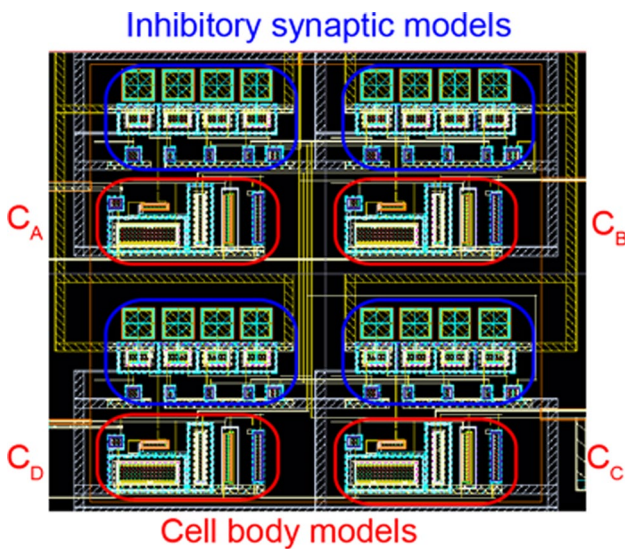
Inhibitory synaptic models

Fig. 4 Layout pattern of the artificial neural networks
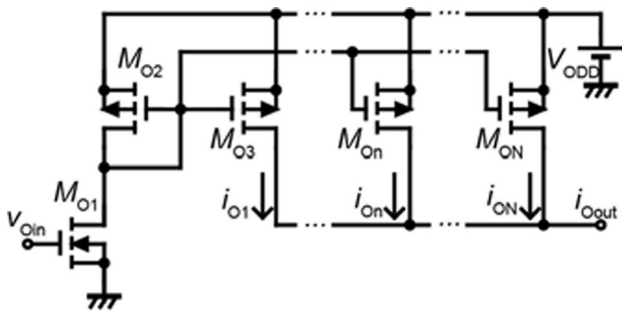
Fig. 5 Circuit diagram of the current output circuit

Fig. 6 Picture of the bare chip IC

Fig. 7 Example of output waveform of bare chip IC

Figure 5 shows the circuit diagram of the current output circuit. The current output circuit outputs the output current i_{Oout} according to the oscillatory waveform v_{Cout} (v_{Oin}). The circuit parameters of the current output circuit were as follows: M_1: $W/L = 40$, M_2: $W/L = 1$, M_{On}: $W/L = 66.7$. In this study, we set as $N = 11$ ($3 \leq \underline{n} \leq N$) because the wire bonding which is the connection between the bare chip IC and the robot could only output 50 mA.

Figure 6 shows the picture of the bare chip IC. We layout several pads to connect to the MEMS microrobot using wire bonding. We layout two pads for each port of microrobot because the driving current of the shape memory alloy-type actuator was larger than the allowable current of the single pad. The sizes of capacitors of the cell body model are too large to implement to the bare chip IC. Therefore, the capacitors C_G and C_M were mounted externally of bare chip IC.

Figure 7 shows the example of the output waveform of designed IC (measured value). Artificial neural networks are coupled neural networks system which could generate the locomotion rhythms such as living organisms. To heat
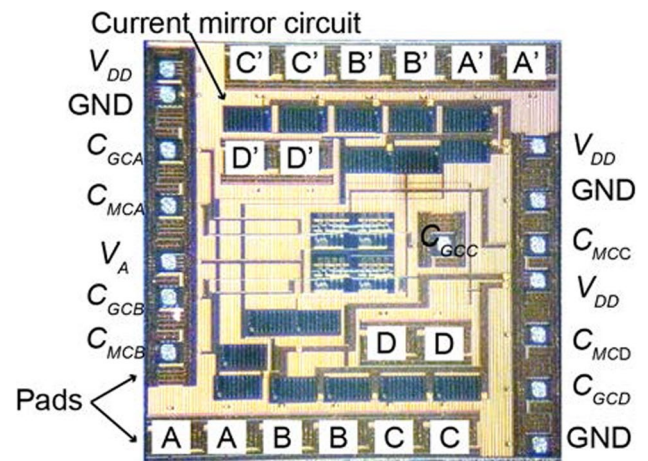
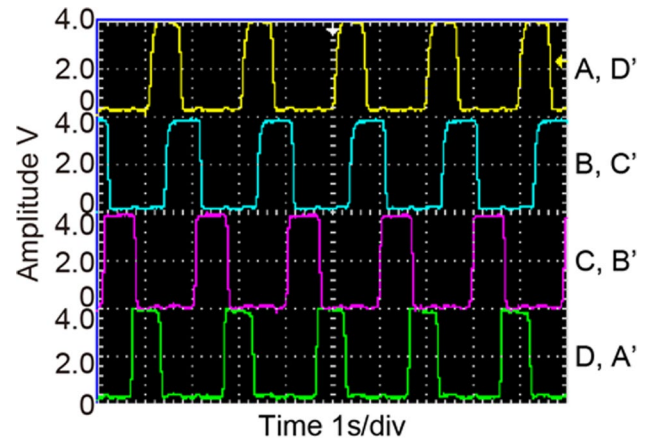the helical artificial muscle wires, we required to input the pulse width 0.5 s, pulse period 2 s and pulse amplitude 75 mA. According to Fig. 7, the output waveform was enough to actuate the actuator of the MEMS microrobot because the resistance of the shape memory alloy-type actuator was about 50 Ω.

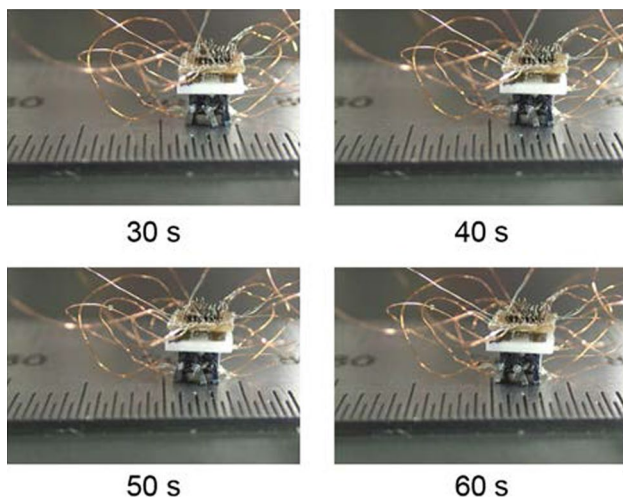## 4 Locomotion of the MEMS microrobot

We mount the bare chip IC of artificial neural networks on top of the MEMS microrobot.

Figure 8 shows the assembled MEMS microrobot system. The MEMS microrobot system was 0.079 g in weight and less than 5.0 mm in size (micro-mechanical system: 0.02 g and micro-electro system: 0.059 g). The weight of the previous micro-electro systems was 0.31 g. We made the reduction of the micro-electro systems in size and weight.

Bare chip IC of artificial neural networks
(Micro-electro systems).
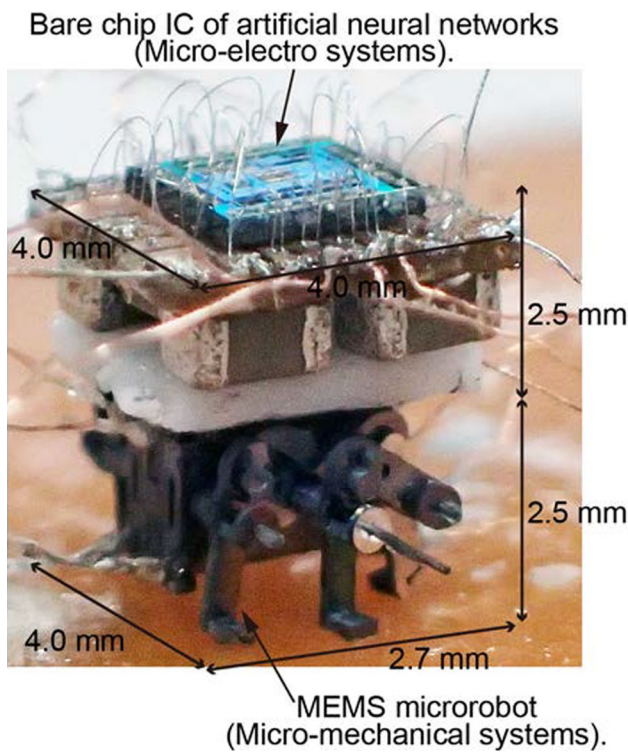
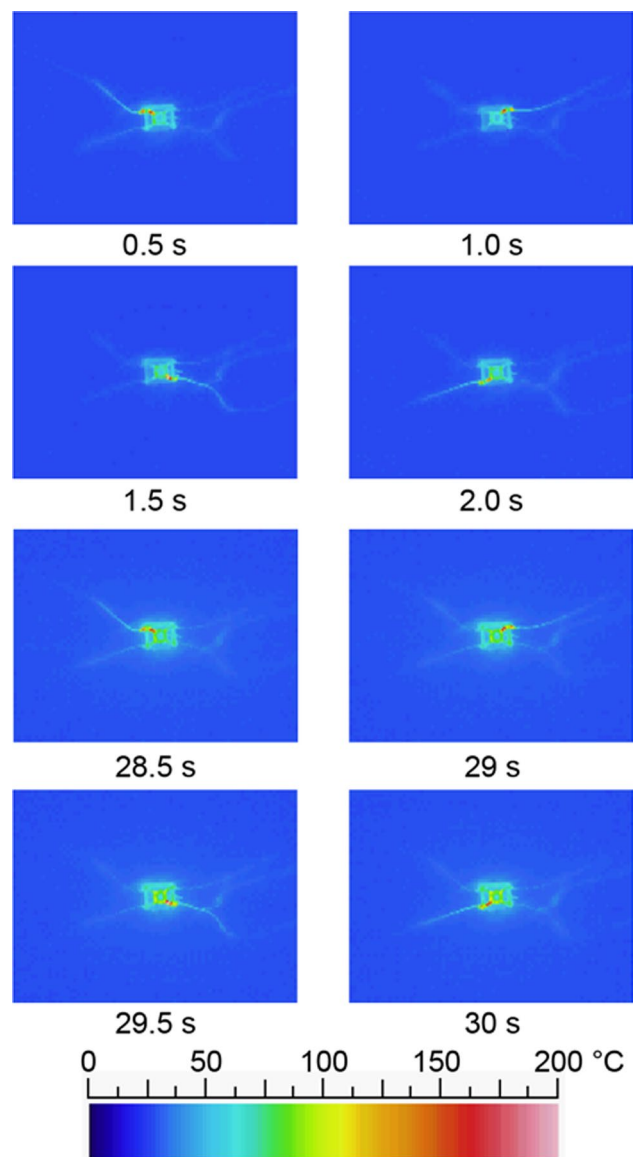**Fig. 8** Assembled MEMS microrobot system

Fig. 9 Example of locomotion of the MEMS microrobot system

Figure 9 shows the example of locomotion of the MEMS microrobot system. Artificial neural networks could output the driving pulse of locomotion which is necessary to actuate the MEMS microrobot. Thus, our artificial neural networks are effective to generate the locomotion of the MEMS microrobot. The locomotion speed of the MEMS microrobot system was 4 mm/min. However, the locomotion speed of the MEMS

microrobot system was too slow as compared with the previous model [18]. The reason of the slow locomotion speed is the heat conduction of the shape memory alloy-type actuator.

Figure 10 shows the heat conduction of the shape memory alloy-type actuator. It was shown that the heat of shape memory alloy conducts to the mechanical parts of the MEMS microrobot. The shape memory alloy shrank at high temperature and extended at low temperature. The heat conduction interferes the radiation of shape memory alloy. Therefore, locomotion becomes slowly after 30 s.

According to the result of Fig. 10, we construct the less conduction shape memory alloy-type actuator. The

Fig. 10 Heat conduction of the shape memory alloy-type actuator
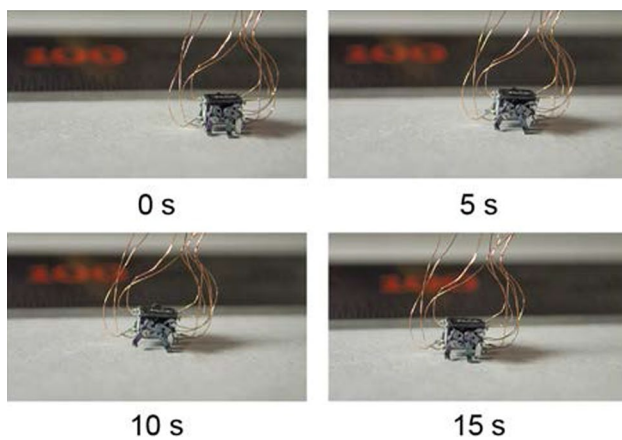
Fig. 11 Example of locomotion of the MEMS microrobot system (less conduction)

locomotion speed of the insect-type MEMS microrobot using less conduction shape memory alloy-type actuator was 90.8 mm/min (Fig. 11).

5 Conclusion

In this paper, we discussed insect-type MEMS microrobot system which could locomote without using computer programs. Locomotion of the MEMS microrobot was generated using the analog circuit of artificial neural networks. We construct the artificial neural networks as a bare chip IC which could mount on top of the MEMS microrobot. As a result, the MEMS microrobot system could perform the locomotion using constructed bare chip IC of artificial neural networks. The insect-type MEMS microrobot system was 0.079 g in weight and less than 5.0 mm in size. In addition, we analyze the heat conduction of the shape memory alloy-type actuator. It was shown that the heat of shape memory alloy conducts to the mechanical parts of the MEMS microrobot; therefore, locomotion will become slowly after 30 s. The locomotion speed of the insect-type MEMS microrobot using less conduction shape memory alloy-type actuator was 90.8 mm/min.

In the future, we will add the sensory system to the MEMS microrobot system.

References

1. Shibata T, Aoki Y, Otsuka M, Idogaki T, Hattori T (1997) Microwave energy transmission system for microrobot. IEICE Trans Electron E80-C(2):303–308
2. Takeda M (2001) Applications of MEMS to industrial inspection. In: IEEE MEMS, pp 182–191
3. Habib MK, Watanabe K, Izumi K (2007) Biomimetics robots: from bio-inspiration to implementation. In: Proceedings of the 33rd annual conference of the IEEE Industrial Electronics Society, pp 143–148
4. Habib MK (2011) Biomimetcs: innovations and robotics. Int J Mechatron Manuf Syst 4(2):113–134
5. Baisch AT, Sreetharan PS, Wood RJ (2010) Biologically-inspired locomotion of a 2g hexapod robot. Proc IEEE IROS 2010:5360–5365
6. Tsuruta K, Mikuriya Y, Ishikawa Y (1999) Micro sensor developments in Japan. Sens Rev 19:37–42
7. Donald BR, Levey CG, McGray CD, Paprotny I, Rus D (2006) An untethered, electrostatic, globally controllable MEMS microrobot. J Microelectromech Syst 15:1–15
8. Edqvist E, Snis N, Mohr RC, Scholz O, Corradi P, Gao J, Johansson S (2009) Evaluation of building technology for mass producible millimeter-sized robots using flexible printed circuit boards. J Micromech Microeng 19(7):1–11
9. Tang WC, Nguyen TH, Howe RT (1989), Laterally driven poly silicon resonant microstructure. In: Proceedings of IEEE micro electro mechanical systems. An investigation of micro structures, sensors, actuators, machines and robots, pp 53–59
10. Sniegowski JJ, Garcia EJ (1996) Surface-micromachined gear trains driven by an on-chip electrostatic microengine. IEEE Electron Device Lett 17:366–368
11. Asada N, Matsuki H, Minami K, Esashi M (1994) Silicone micromachined two-dimensional galvano optical scanner. IEEE Trans Magn 30:4647–4649
12. Suzuki Y, Tani K, Sakuhara T (2000) Development of a new type piezoelectric micromotor. Proc Sens Actuators A: Phys 83:244–248
13. Surbled P, Clerc C, Pioufle BL, Ataka M, Fujita H (2001) Effect of the composition and thermal annealing on the transformation temperature sputtered TiNi shape memory alloy thin films. Thin Solid Films 401:52–59
14. Matsuoka K (1987) Mechanism of frequency and pattern control in the neural rhythm generators. Biol Cybern 56:345–353
15. Ikemoto T, Nagashino H, Kinouchi Y Yoshinaga T (1997) Transitions in a four coupled neural oscillator model. In: International symposium on nonlinear theory and its applications, pp 561–564
16. Nakada K, Asai T, Amemiya Y (2003) An analog CMOS central pattern generator for interlimb coordination in quadruped locomotion. IEEE Trans Neural Netw 14:1356–1365
17. Okazaki K, Ogiwara T, Yang D, Sakata K, Saito K, Sekine Y, Uchikoba F (2011) Development of pulse control type MEMS micro robot with hardware neural network. Artif Life Robot 16(2):229–233
18. Saito K, Takato M, Sekine Y, Uchikoba F (2012) Biomimetics micro robot with active hardware neural networks locomotion control and insect-like switching behaviour. Int J Adv Robot Syst In Tech 9(226):1–6
19. Maezumi K, Yamasaki S, Obara H, Naito Y, Iwata K, Tatani M, Okane Y, Ishihara Y, Hidaka T, Asano Y, Oku H, Takato M, Saito K, Uchikoba F (2014) Hexapod-type SMA driven MEMS microrobot with mounted bare chip artificial neural networks IC. In: Proceedings of the nineteenth international symposium on artificial life and robotics 2014, pp 401–405

20. Bhardwaj JK, Ashraf H (1995) Advanced silicon etching using high-density plasmas. In: Proceedings of SPIE micromachining and micro fabrication process technology, vol 2639, pp 224–233

21. Homma D (2003) Metal artificial muscle bio metal fiber. RSJ 21:22–24

22. Toki Corporation's Homepage. http://www.toki.co.jp. Accessed 24 Dec 2015